MATERIALS PROCESSING FUNDAMENTALS 2020

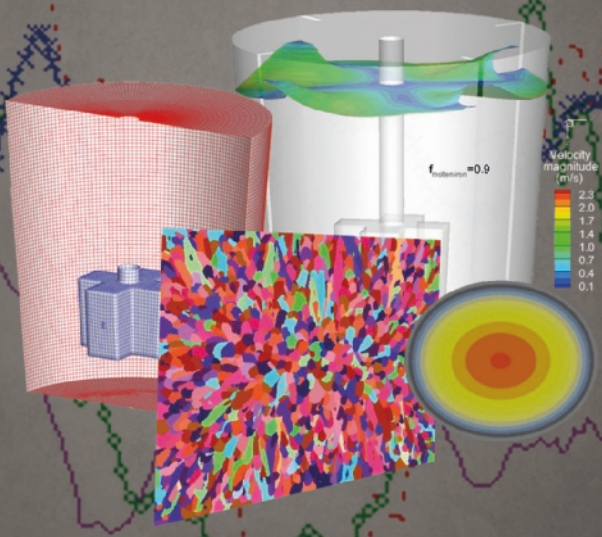

EDITED BY
Jonghyun Lee
Samuel Wagstaff
Guillaume Lambotte
Antoine Allanore
Fiseha Tesfaye

TMS
Springer

The Minerals, Metals & Materials Series

Jonghyun Lee · Samuel Wagstaff ·
Guillaume Lambotte · Antoine Allanore ·
Fiseha Tesfaye
Editors

Materials Processing Fundamentals 2020

TMS

Springer

Editors
Jonghyun Lee
Iowa State University
Ames, IA, USA

Guillaume Lambotte
Boston Metal
Woburn, MA, USA

Fiseha Tesfaye
Åbo Akademi University
Turku, Finland

Samuel Wagstaff
Novelis
Kennesaw, GA, USA

Antoine Allanore
Massachusetts Institute of Technology
Cambridge, MA, USA

ISSN 2367-1181 ISSN 2367-1696 (electronic)
The Minerals, Metals & Materials Series
ISBN 978-3-030-36555-4 ISBN 978-3-030-36556-1 (eBook)
https://doi.org/10.1007/978-3-030-36556-1

Cover illustration: Left and top right: From Chapter "Numerical Simulation on the Multiphase Flow During the KR Process Using the Eulerian–Eulerian Modeling", Yanyu Zhao et al., Figure 1: Calculation domain geometry (a) and mesh distribution (b) and Figure 5: Free surface distribution under different conditions, (a) without gas injection, (b) with gas injection, (c) with baffle, and (d) with slope bottom. https://doi.org/10.1007/978-3-030-36556-1_15. Bottom right and bottom left: From Chapter "Control Center Segregation in Continuously Cast GCr15 Bloom by Optimization of Solidification Structure", Hanghang An et al., Figure 6: Simulated results of (a) fraction solid distributions and (b) morphologies of bloom samples with steel nails and Figure 16: Simulated solidification structure of central equiaxed grain zone: (a) without M-EMS; (b) with M-EMS. https://doi.org/10.1007/978-3-030-36556-1_18.

This Springer imprint is published by the registered company Springer Nature Switzerland AG
The registered company address is: Gewerbestrasse 11, 6330 Cham, Switzerland

Contents

Part VI Poster Session

About the Editors

Jonghyun Lee is Assistant Professor in the Department of Mechanical Engineering at Iowa State University. He has been conducting multiple industry and government-funded projects in the field of materials processing as PI and Co-PI. He is the recipient of the Young Leaders Professional Development Award in 2013 from The Minerals, Metals & Materials Society where he has been serving as a Co-organizer and Co-editor of the Materials Processing Fundamentals Symposium since 2014 and as Vice-Chair of the Process Modeling and Technology Committee since 2017. Prior to joining his current institution, he was a Research Assistant Professor at the University of Massachusetts, Amherst. He also had nearly 5 years of industry experience and worked as a Post-doctoral Associate for Tufts University, Medford, Massachusetts. He earned his M.S. and Ph.D. in Mechanical Engineering from the University of Massachusetts Amherst and his B.S. in the same discipline from Inha University in Incheon, South Korea.

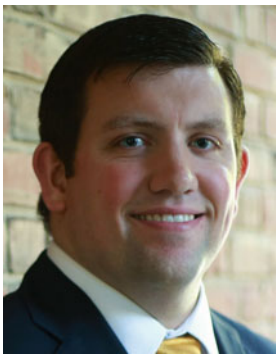

Samuel Wagstaff began working in the aluminum industry at age 14 with Novelis in Spokane, Washington and now works for the same company in Kennesaw, Georgia as a Process Scientist. In 2013, he received his Bachelor of Science from Cornell University in Mechanical and Aerospace Engineering. He continued his education at the Massachusetts Institute of Technology in the Department of Materials Science and Engineering. His Ph.D. on the minimization of macrosegregation through jet erosion of a continuously cast ingot uses a turbulent jet to reduce the uneven distribution in aluminum alloy ingots by over 70%. He finished his masters and doctorate at MIT in September 2016 after just 3 years. He has published more than a dozen articles on DC casting and macrosegregation and holds 12 patents.

Guillaume Lambotte is R&D Director at Boston Metal, a Massachusetts Institute of Technology (MIT) spin-off startup focusing on the development of an environmentally friendly and energetically efficient primary metal extraction process. Dr. Lambotte primarily focuses on computational thermodynamic modeling, electrochemistry, and high-temperature equilibrium. Prior to joining Boston Metal, he conducted research as a post-doctoral associate at the University of Massachusetts Amherst and MIT. Before his graduate studies, Dr. Lambotte worked as a production assistant manager at Alcan Extruded Products (Crailsheim, Germany).

Dr. Lambotte obtained his bachelor's degree from the European Engineer School for Materials Science (Nancy, France). He received an M.Sc. and a Ph.D. in metallurgical engineering from Ecole Polytechnique of Montreal (Montreal, Canada).

Dr. Lambotte was the recipient of the 2015 TMS EPD Young Leaders Professional Development Award. The same year he was one of the TMS representatives at the Emerging Leaders Alliance Conference.

Antoine Allanore is Associate Professor of Metallurgy in the Department of Materials Science & Engineering at MIT. He received his higher education in Nancy (France) where he earned a chemical process engineer diploma from Ecole Nationale Supérieure des Industries Chimiques and an M.Sc. and Ph.D. from Lorraine University. Dr. Allanore joined MIT in 2012 as a faculty member, leading a research group that develops sustainable materials extraction and manufacturing processes. He has developed numerous alternative approaches for metals and minerals extraction and processing. With an emphasis on electrochemical methods for both analytical and processing purposes, his group combines experimental and modeling approaches to promptly investigate the ultimate state of condensed matter, the molten state. He teaches thermodynamics and sustainable chemical metallurgy at both the undergraduate and graduate levels. He received the Vittorio de Nora Award from TMS in 2012 and the TMS Early Career Faculty Fellow Award in 2015.

Fiseha Tesfaye is Senior Researcher and Adjunct Professor in metallurgical thermodynamics at the Johan Gadolin Process Chemistry Centre (PCC) of Åbo Akademi University, Finland. He received his master's degree in materials processing technology in 2009 from Helsinki University of Technology and his Ph.D. degree in metallurgy in 2014 from Aalto University, Finland. During his Ph.D. period, he focused his research on the electrochemical investigation of the thermodynamic properties of sulfide and intermetallic materials.

After a post-doctoral position in the Laboratory of Inorganic Chemistry at Åbo Akademi University from 2015 to 2017, which was focused on the sulfosalts and sulfates characterizations, Dr. Tesfaye attracted a large research project related to the thermodynamic investigation of complex inorganic material systems in renewable energy and metal production processes. From September 2017 onward, his research activities have been focused mainly on the sulfate-oxide systems database development with the FactSage software package, as well as rigorous theoretical and experimental investigations for promoting improved recovery

of values from waste streams. Dr. Tesfaye was also appointed as a Visiting Research Scientist at Seoul National University, South Korea, for 6 months between March and August 2018. His current research interests are also within the scope of metallurgical engineering and circular economy of metals.

Dr. Tesfaye is a regular contributor and member of TMS and is the 2018 TMS Young Leaders Professional Development Award winner. He has served on TMS committees including Recycling and Environmental Technologies, Energy, and Professional Development. He has edited scientific research books and has served as a guest editor for *JOM*. His personal achievements include significant improvement of experimental research applying the solid-state EMF technique for thermodynamic studies, as well as contribution of new experimental thermodynamic data of several chalcogenide materials. He has published more than 40 peer-reviewed articles.

Part I
Nucleation, Crystallization, and Solidification

Demineralization of a High Ash Coal in Acidic Salt Solution

A. A. Adeleke, L. O. Jimoh and S. A. Ibitoye

Abstract The research investigated the reduction of the ash and sulphur contents of the high ash and high sulphur Nigerian Akunsa coal. The coal as received contained 38 and 1.98% of ash and sulphur, respectively. The coal samples were leached using sodium carbonate, nitric acid, and sodium carbonate acidified in nitric acid at varying combinations of concentrations, contact time, and at a constant temperature of 90 °C. The results obtained showed that sulphur and ash were effectively removed by nitric acid and sodium carbonate, respectively. It was further observed that the 1.5 M sodium carbonate acidified in 1 M nitric acid gave the highest leaching efficiency for the same solid-to-liquid ratio as the ash was reduced by 76.8–8.8% and the sulphur reduced by 82.3–0.35%. The coal concentrate obtained contains permissible ash and sulphur that render it suitable for blending in cokemaking.

Keywords Coal · High ash · High sulphur · Leaching · Concentrate

Introduction

Coal is a combustible fossil fuel and a sedimentary organic rock which is composed mainly of carbon, hydrogen, and oxygen. Coals with high ash content requires higher transport cost and also increases erosion in plant parts, which makes coal grinding difficult, lowers flame temperature, and thus increases energy requirement. The use of coals with lower ash has been found to reduce plant parts erosion rates by more than 50% and maintenance costs by 35%, an increase in thermal efficiency by 4–5% in pulverized coal boilers, and reduction in carbon dioxide emissions by 15%. Fluidized bed combustors have also been found to operate more efficiently with higher grade coals [1].

The chemical leaching methods to reduce ash and sulphur contents of coals include molten caustic leaching and agitation caustic leaching, mineral acid leaching and have been successfully employed to reduce the ash and sulphur contents of coals [2, 3]. Nigeria is endowed with coal deposits such as those of Lafia-Obi and Akunsa

A. A. Adeleke (✉) · L. O. Jimoh · S. A. Ibitoye
Department of Materials Science and Engineering, Obafemi Awolowo University, Ile-Ife, Nigeria
e-mail: abrahamadeleke@gmail.com

J. Lee et al. (eds.), *Materials Processing Fundamentals 2020*, The Minerals, Metals & Materials Series, https://doi.org/10.1007/978-3-030-36556-1_1

in Nassarawa state in the north central region of the country. The coal deposits are found in the middle region of the Benue trough, a sedimentary basin stretching about 1000 km long from the Gulf of Guinea to the Lake Chad basin. While the Lafia-Obi deposit had been extensively explored and found to hold about 22 million tons of coal, the Akunsa deposit reserve estimate is not available [4].

In this research, the high ash and high sulphur Akunsa coal was effectively demineralized in sodium carbonate acidified with nitric acid.

Materials and Methods

Materials

Sample Preparation

About 3.5 kg of Akunsa coal lumps was received for the laboratory-scale research. The coal lumps were crushed, air dried, and properly ground manually and later homogenized in a mortar by pounding with a pestle.

Methods

Particle Size Analysis Using Sieving Method

The sizing ground coal sample was carried out by employing sieves and an automated vibrating sieve shaker. The sieves were selected based on the square root of two rules. The weights of the sieves—355, 250, 150, 125, and 90 μm were taken empty and stacked in that decreasing order of mesh size with a collecting pan at the bottom. 200 g of the crushed and ground coal sample was poured into the uppermost coarsest sieve, and the stack sieves was shaken in a vertical plane for 60 min. After the required time, the stack of sieves was taken apart, and the mass of coal retained on each sieve was weighed.

Proximate Analysis

Proximate analysis was carried out on both the representative sample and the leached Akunsa coal to determine their weight per cent moisture content, ash, volatile, and fixed carbon content using modified ASTM methods.

Preparation of Leach Solutions

1.5 M solution of sodium carbonate was prepared. The 1 and 0.5 M solutions were then produced from the 1.5 M solution by serial dilution. 1.5 M of nitric acid solution was also produced, and 1 and 0.5 M solutions were produced from it by serial dilution.

Leaching Demineralization Tests

Atmospheric leaching in oven

The coal sample was subjected to leaching at atmospheric pressure in the oven and on the magnetic stirrer hot plate using 3^2 factorial design as shown in Table 1, with reagent concentration and contact time varied at three levels while the temperature was held constant at 90 °C. The reagent concentrations of $C_1 = 1.5$, $C_2 = 1$, and $C_3 = 0.5$ M and contact times of $t_1 = 30$, $t_2 = 60$, and $t_3 = 90$ min were used.

One gram of coal sample was weighed on a clean watch glass and transferred into a clean conical flask containing 25 ml of the prepared solution. The slurry in the conical flask was then homogenized by stirring for 5 min, covered with Al foil and transferred into the oven for leaching in combinations shown in Table 1. The resulting concentrates were skimmed off, air dried for 48 h, oven dried at 105 °C for 60 min, and weighed. The leaching was further repeated in the oven with the t_3C_3 leaching combination that gave the highest weight loss but using 0.25, 0.5, 0.75, 1.0, and 1.5 M sodium carbonate solutions acidified with 1 M nitric acid.

The leaching on magnetic stirrer hot plate was carried out by selecting the t_3C_3 combination and that of acidic mixture that gives the best reduction in mineral matter. One gram of coal sample was weighed and transferred into a clean conical flask containing 25 ml of prepared solution of t_3C_3 combination and 1.5 M sodium carbonate acidified with 1 M nitric acid. The slurry in the conical flask was then homogenized

Table 1 Factorial combination of time and concentration for atmospheric oven leaching

S/N	Time (min)	Concentration (M)	Combinations
1	t_1	C_1	t_1C_1
2	t_1	C_2	t_1C_2
3	t_1	C_3	t_1C_3
4	t_2	C_1	t_2C_1
5	t_2	C_2	t_2C_2
6	t_2	C_3	t_2C_3
7	t_3	C_1	t_3C_1
8	t_3	C_2	t_3C_2
9	t_3	C_3	t_3C_3

by stirring for 5 min, covered with Al foil and heated for leaching. Leaching experiments were conducted on magnetic stirrer at constant temperature of 90 °C and for 30 min contact time. The temperature was monitored with a thermometer. The resulting concentrate was skimmed off, air dried, oven dried, and weighed.

Determination of Total Sulphur by Eschka Method

The determination was carried out as described by Francis and Peters [5].

Results and Discussion

The results obtained showed that 30.40% of the coal was retained on the sieve size 355 μm after crushing and grinding. This suggests that the coal is relatively hard and thus respond slowly to crushing and grinding as less than 70% pass the relatively coarse 355 μm sieve size. The results obtained for moisture, volatile matter, ash, and fixed carbon of the coal sample are presented in Table 2. The high ash content of 38% for the coal as received showed that Akunsa coal is a high ash coal whose ash content far exceeds the maximum of 10% allowed in coals for use in metallurgical cokemaking [6]. A low-quality, high ash coal creates problems in both ironmaking and power generation. For instance, in India, it has been found that the supply of high ash coals with 30–50% ash causes increased transport cost due to the carriage of large amounts of ash forming minerals and creates shortages of rail cars and port facilities.

A high ash coal aggravates erosion in plant parts, makes coal pulverization difficult, lowers flame temperature and radiative heat transfer, and leads to production of excessive amount of fly ash containing large amounts of un-burned carbons. The use of beneficiated coal has been found to cause a reduction in erosion rates by 50–60% and maintenance costs by 35%, an increase in thermal efficiency by 4–5% in pulverized coal boilers, and reduction in carbon dioxide emissions by 15%. Even fluidized bed combustors have been found to operate more efficiently with higher grade coals [1].

Table 2 Proximate analysis of Akunsa coal

Parameter	% Content
Moisture	4.4
Volatile matter	10.2
Ash	38
Sulphur	1.98
Fixed carbon	47.4

Coal beneficiation has been found to be a low-cost solution for high ash Indian coals and a means of reducing imports of high grade foreign coals. Raw coals for power generation are cleaned to contain below 34% ash. The Indian Dadri power plant uses 34–35% ash coal from Indian Central Coalfield Limited. Typical landing cost of Run of Mine (ROM) high ash Indian coal is $38.80/ton and transport over 400 km cost $26.10/ton [1]. Considering the detrimental effects of high ash in coals for coal transport, cokemaking, and combustion for power generation, it is necessary to reduce the ash content of the Akunsa coal.

The sulphur content was determined to be 1.98% for the coal as received. The results obtained showed that the sulphur content of the Akunsa coal is much higher than the maximum of 0.9% required for coals for cokemaking [6]. High sulphur in coke on combustion forms sulphur dioxide, a very strong oxidizing agent. Additionally, an appreciable amount of sulphur in coke passes into the molten iron. This reduces the quality of the iron in terms of mechanical strength, and the oxidizing nature of the sulphur dioxide complicates the operations of subsequent conversion of iron to steel [5, 7].

The results obtained on the leaching of the Akunsa coal samples with solutions of sodium carbonate, nitric acid, and their mixture are presented in Figs. 1, 2, and 3, respectively. The results obtained showed that for the same leaching duration of 30, 60, or 90 min, the percentage weight loss in the samples was highest at the highest sodium carbonate molar concentration of 1.5 M with about 15% decrease in weight. Similarly, the results for 1.5 M nitric acid gave the highest weight loss of 6% at 90 min compared to the 15% for sodium carbonate, while the sodium carbonate acidified with nitric gave a much higher weight loss of 19% for the same leaching conditions at 1.5 M sodium carbonate solution. Thus, the weight loss obtained generally increased with increasing contact time and increasing concentration of the two leachants.

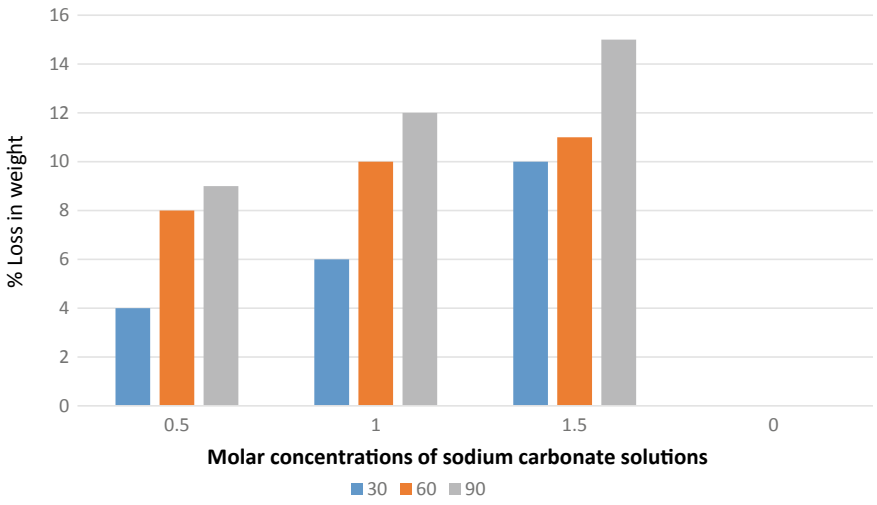

Fig. 1 Percentage weight loss in coal after sodium carbonate atmospheric oven leaching

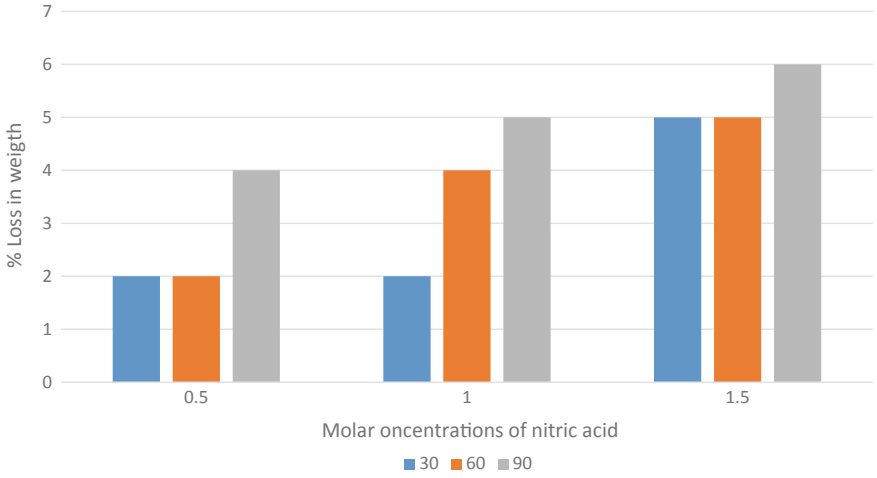

Fig. 2 Percentage weight loss in coal in nitric acid atmospheric oven leaching

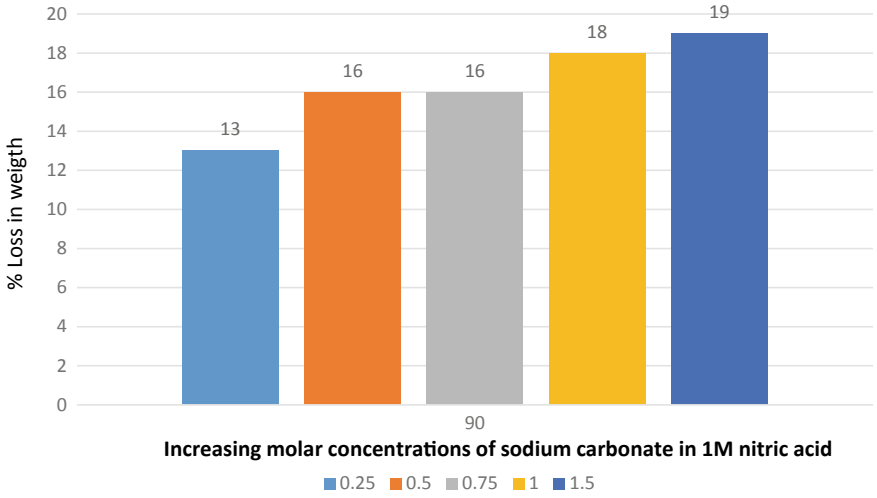

Fig. 3 Percentage weight loss in coal in acidified sodium carbonate atmospheric oven leaching

The results further showed that nitric acid is a weaker leachant for Akunsa coal than sodium carbonate as it gave a much lower 6% weight loss for the coal as against 15% for sodium carbonate at the same 1.5 M molar concentration and 90 min contact time. However, sodium carbonate in acidified solution of nitric is much stronger than nitric acid alone and gave 19% weight loss at 1.5 M sodium carbonate and 90 min contact time. The reduction in weight of the sample showed that the leaching was effective as part of the coal material was successfully converted to solution to remove them from the coal.

The higher weight loss in the acidified sodium carbonate may due to the increase in the reacting potency of sodium carbonate in the presence of nitric acid. The increasing weight loss at higher molar concentrations may be due to increasing collision between coal particles and the sodium carbonate ionic species at higher concentration. It has been established that leaching rate increases with increasing leachant concentration [8].

The results obtained for leaching on the magnetic stirrer hot plate with its agitating follower and a temperature of about 90 °C showed that weight losses of 26, 37, and 51% were obtained for the agitating leaching of Akunsa coal with nitric acid, sodium carbonate, and the mixture, respectively (Fig. 4). The weight losses were much higher than for oven leaching for all the reagent options used on the hot plate. The results showed that the effect of pulp agitation was very high on the leaching rate. Pulp stirring has been established as an important parameter for effective leaching [8].

The ash contents determined for the coal as received, the coal as leached by sodium carbonate solution, the coal as leached by nitric acid, and the coal as leached by sodium carbonate acidified in nitric acid by atmospheric oven and on magnetic stirrer hot plate leaching are shown in Tables 3 and 4, respectively. The results obtained gave 38% for the Akunsa coal as received and 19.7, 29.3, and 14.9%, respectively, for the coal oven leached by sodium carbonate solution, nitric acid solution, and sodium carbonate acidified in nitric acid. The agitation leaching on the magnetic stirrer yielded coal concentrates with 11.2, 19.2, and 8.8% ash contents, respectively. The results obtained translate to ash reduction per cents of 22.9, 48.2, and 60.8; and 49.5, 70.5, and 76.8% for oven and magnetic stirrer leaching, respectively.

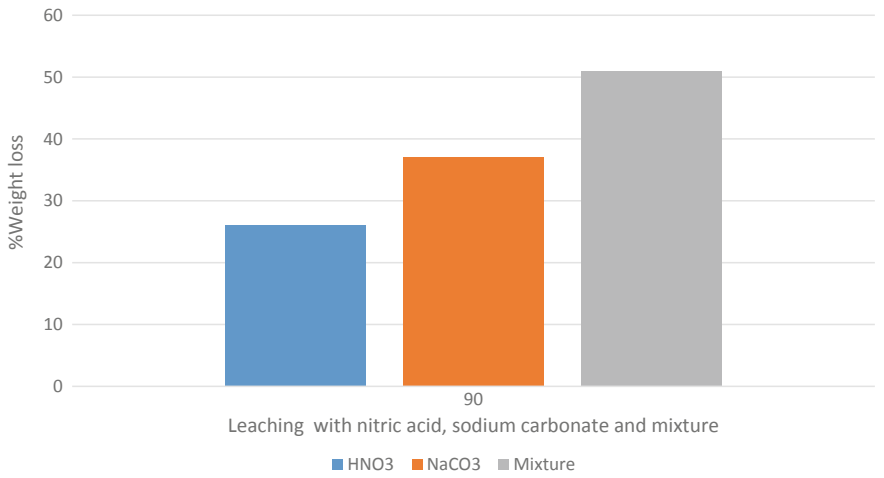

Fig. 4 Percentage weight loss in coal on magnetic stirrer for nitric, sodium carbonate, and acidified sodium carbonate after 30 min

Table 3 Ash content in leached coal in atmospheric oven and magnetic stirrer leaching

Leachant	% Ash after oven leaching	% Ash reduction	% Ash after agitation leaching	% Ash reduction
Nitric acid (1.5 M, 90 min)	29.3	22.9	19.2	49.5
Sodium carbonate (1.5 M, 90 min)	19.7	48.2	11.2	70.5
Mixture (1 M nitric acid, 1.5 M SC, 90 min)	14.9	60.8	8.8	76.8

Table 4 Effect of sodium carbonate, nitric acid, and acidic mixture on Akunsa coal sulphur in atmospheric oven and agitation leaching

Leachant	% S after oven leaching	% S reduction	% S after agitation leaching	% S reduction
Nitric acid (1.5 M, 90 min)	0.99	50	0.82	58.6
Sodium carbonate (1.5 M, 90 min)	1.38	30.3	1.14	42.4
Mixture (1 M nitric acid, 1.5 M SC, 90 min)	0.93	53	0.35	82.3

Similarly, the sulphur contents determined for the Akunsa coal as received were 1.98% and 0.99, 1.38 and 0.94%, respectively, for the coal oven leached by nitric acid solution, sodium carbonate solution, and sodium carbonate solution acidified in nitric acid, respectively. The agitation leaching on the magnetic stirrer yielded coal concentrates with 1.15, 0.82, and 0.36% sulphur contents, respectively. The results translate to sulphur reduction per cents of 50.0, 30.3 and 58.60 and 42.40 and 82.30%, respectively. The results obtained thus showed that sodium carbonate was more efficient than nitric acid in ash reduction, while nitric acid was more effective in sulphur removal. The theory of the leaching is that sodium carbonate reacts with ash components such as silica, iron oxide, and alumina to form water-soluble complex silicates like sodium silicate, sodium aluminium silicate, and others. It also forms soluble compounds of sulphur to reduce the sulphur content. Nitric acid also reacts with ash components and sulphur to form water-soluble compounds thus reducing the ash and sulphur contents.

Conclusion

The high ash and high sulphur Akunsa coal was successfully demineralized of its ash and sulphur contents using sodium carbonate, nitric acid, and sodium carbonate acidified with nitric acid in the oven and on the magnetic stirrer hot plate. However, the results obtained showed that sodium carbonate acidified with nitric acid gave the best concentrate during agitation leaching and reduced the ash content by 76.80% and sulphur by 82.30%.

References

1. Zamuda CD, Sharp MA (2007) A case for enhanced use of clean coal in India. https://fossil.energy.gov›Publications›coal_beneficiation_paper_zamuda. Accessed 5th Sept 2019
2. Adeleke AA, Ibitoye SA, Afonja AA (2013) Multistage caustic leaching de-sulphurization of a high sulphur coal. P&C 55(2):544–551
3. Adeleke AO, Makan RS, Adahama AB, Makan RS, Ibitoye SA (2007) An evaluation of the coking characteristics of Polish coking coals for cokemaking with non-coking Nigerian coals. P&C 49(1):1–6
4. Federal Ministry of Mines and Steel Development (2005) Coal exploration and power generation opportunities in Nigeria. http://www.mmsd.gov.ng/Downloads/Coal.pdf. 27th Nov 2010
5. Francis W, Peters MC (1980) Fuels and fuel technology. Pergamon Press, New York
6. Raw Materials and products specifications (1994) For Federal Government Steel Companies, Nigeria
7. Krivandin V, Markov B (1980) Metallurgical furnaces. Mir Publishers, Moscow
8. Ghosh A, Ray HS (1991) Principles of extractive metallurgy. Wiley, New York

Simulation for Solidification Structure of Continuous Casting Bloom Using Cellular Automaton-Finite Element Model

Yadong Wang, Dongbin Jiang, Sha Ji and Lifeng Zhang

Abstract A coupled cellular automaton-finite element (CAFE) model was used to simulate the solidification structure of continuous casting bloom. The simulated solidification structure and temperature field were validated by the industrial trial. The influence of superheat, secondary cooling water flow, and mold electromagnetic stirring (M-EMS) on the solidification structure was discussed. To simulate the intense flow field and uniform temperature with M-EMS, the thermal conductivity in liquid and the formation of crystals increased, separately. The ratio of equiaxed crystal zone decreases from 28.47 to 16.45% with the superheat increasing from 15 to 35 °C. With the secondary cooling water flow increasing 20% and decreasing 20%, the ratio of equiaxed crystal zone is 20.64% and 23.16%, respectively. The ratio of equiaxed crystal zone increases from 21.75 to 32.77% with the application of M-EMS.

Keywords Solidification structure · CAFE method · Mold electromagnetic stirring · Superheat · Secondary cooling water flow

Introduction

Solidification structure during continuous casting process has a significant effect on the internal quality of the final steel products especially for the internal cracks, macrosegregation, porosity, and so on. Homogenization heat treatment and rolling process are impossible to eliminate internal defects of bloom [1, 2]. Therefore, solidification structure should be properly controlled by optimizing the continuous casting parameters.

With the improvement of computational efficiency and solidification structure models, the simulation of solidification structure can be achieved. There are two main simulation methods including deterministic models and stochastic models [3,

Y. Wang · D. Jiang · S. Ji · L. Zhang (✉)
School of Ecological and Metallurgical Engineering, University of Science and Technology Beijing, Beijing 100083, China
e-mail: zhanglifeng@ustb.edu.cn

J. Lee et al. (eds.), *Materials Processing Fundamentals 2020*, The Minerals, Metals & Materials Series, https://doi.org/10.1007/978-3-030-36556-1_2

4]. The cellular automaton-finite element (CAFE) model is one of the stochastic models which was widely used in the last decades. Rappaz and Gandin [3] are the earliest researchers who simulated the microstructure of Al alloy using CAFE method. Thereafter, the CAFE method was gradually utilized in the continuous casting process [4–6]. Based upon a two-dimensional cellular automaton (CA) technique, Rappaz et al. [3] investigated the effect of the cooling rate upon the microstructure. The extent of the columnar region is reduced with the increasing of cooling rate. Gandin et al. [7] established a 3-D CAFE model for the prediction of dendritic grain structures formed during solidification. It was demonstrated that the 3-D CAFE model was feasible for the investment casting and continuous casting processes. Zhang et al. [8] studied the effects of undercooling, casting temperature, mold initial temperature, and filling rate on the solidification structure of the ingot based on a 3-D CA method. The undercooling is a critical parameter on the solidification; however, the initial temperature of the mold has little effect on the final solidification structure. Fang et al. [6] utilized the CAFE model to discuss the effect of secondary cooling conditions and superheat on the solidification structure of continuous casting bloom. The results shown that the secondary cooling conditions had little effect on the grain size and the percentage of center-equiaxed grains decreased with the superheat increasing.

In the current work, the CAFE model validated by trial results was used to simulate the solidification structure of continuous casting bloom. The effect of superheat, secondary cooling water flow, and M-EMS on the solidification structure was discussed.

Mathematical Formulation

The content of the 20CrMnTi bloom is listed in Table 1. The main parameters used in the current study are listed in Table 2.

In the current model, the nucleation and grain growth were calculated by the CA method in which the Gaussian distribution of nucleation was used. The continuous heterogeneous nucleation model was used in the CA method and was expressed by Eq. (1).

$$\frac{\mathrm{d}n}{\mathrm{d}(\Delta T)} = \frac{n_{\max}}{\sqrt{2\pi}\Delta T_{\sigma}} \exp\left[-\frac{(\Delta T - \Delta T_{\mathrm{ave}})^2}{2\Delta T_{\sigma}^2}\right] \tag{1}$$

where ΔT is undercooling in K; $n_{\max}$ is the maximum nucleation density in m^{-3}; ΔT_{σ} is the standard deviation in K; ΔT_{ave} is the mean undercooling in K. The growth

Table 1 Chemical compositions of 20CrMnTi bloom

Elements	C	Si	Mn	P	S	Cr	Ti	Al
Content (%)	0.20	0.24	0.89	0.02	0.01	1.09	0.06	0.02

Table 2 Parameters of continuous casting process

Parameters	Values
Bloom dimension (mm^2)	510 × 390
Effective mold length (mm)	680
Submerged depth of SEN (mm)	90
Casting speed (m/min)	0.42
Pouring temperature (K)	1811
Liquidus temperature of molten steel (K)	1786
Solidus temperature of molten steel (K)	1723

velocity of dendrite tip was calculated according to the simplified Kurz–Giovanola–Trivedi (KGT) model [8, 9].

$$V(\Delta T) = a_2 \Delta T^2 + a_3 \Delta T^3 \tag{2}$$

where a_2, a_3 are the fitting polynomial coefficients of the dendrite tip growth kinetic parameters. In current calculation, a_2, a_3 are 0.0 and 8.031×10^{-6}, respectively; $V(\Delta T)$ is the growth velocity of the dendrite tip.

The heat transfer during continuous casting was calculated by finite element (FE) model, and the governing equation was expressed by Eq. (3).

$$\frac{\partial T}{\partial t} = \frac{\lambda}{\rho C_\mathrm{p}} \left(\frac{\partial^2 T}{\partial x^2} + \frac{\partial^2 T}{\partial y^2} \right) \tag{3}$$

where λ is the thermal conductivity in W/(m K), ρ is the density in kg/m^{-3}, and C_p is specific heat in J/(kg K). The procedure of CAFE model was as follows: The temperature field was calculated using coarse mesh, and then to combine the FE and CA calculation in the same model, the FE elements were subdivided into much smaller grids to ensure the calculating precision of the nucleation and growth. The latent heat released in the nucleation and growth progress was fed back to the thermal calculation, updating the temperature of the nodes in FE model. Finally, the CA and FE model were fully coupled [3, 10].

To improve the computational efficiency, a moving slice model was established [4]. From the meniscus to the cutting point, different cooling boundary conditions were applied to the model, shown in Table 3 [11, 12]. The parameters used in the CAFE model are shown in Table 4, where $\Delta T_{\mathrm{v,ave}}$ is the mean undercooling of internal nucleation, $\Delta T_{\mathrm{v},\sigma}$ is the standard deviation of internal nucleation, $n_{\mathrm{v,max}}$ is the maximum nucleation density of internal nucleation, $\Delta T_{\mathrm{s,ave}}$ is the mean undercooling of surface nucleation, $\Delta T_{\mathrm{s},\sigma}$ is the standard deviation of surface nucleation, and $n_{\mathrm{s,max}}$ is the maximum nucleation density of surface nucleation.

Table 3 Governing equations of cooling conditions

Cooling zone	Boundary conditions	Governing equations
Mold	q	$q = 2680000 - 315000\sqrt{t}$
Foot roller section	$q_s = h_s(T - T_w)$	$h = 5849.9 \times W^{0.451} \times (1 - 0.0075\theta)$
Section 2 in secondary cooling zone		
Section 3 in secondary cooling zone		
Section 4 in secondary cooling zone		
Section 5 in secondary cooling zone		
Air cooling zone	$q_a = \varepsilon\sigma(T^4 - T_a^4)$	$\varepsilon = 0.8$

Table 4 Parameters in the CAFE model

Parameters	$\Delta T_{v,ave}$ (K)	$\Delta T_{v,\sigma}$ (K)	$n_{v,max}$ (m^{-3})	$\Delta T_{s,ave}$ (K)	$\Delta T_{s,\sigma}$ (K)	$n_{s,max}$ (m^{-2})
Value	2.0	0.6	6.5×10^8	1.0	0.1	1.0×10^8

Model Validation

In the current study, the temperature field was calculated by the FE model. Obviously, the simulated temperature in the loose side center was agreement with the measured ones shown in Fig. 1. The comparison of the numerical and trial solidification structures without mold electromagnetic stirring (M-EMS) was shown in Fig. 2. The ratio of equiaxed crystal zone in calculation and industrial experiment

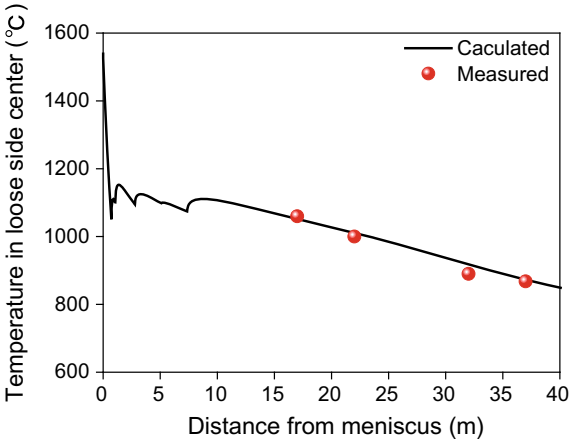

Fig. 1 Simulated and measured temperature in loose side center

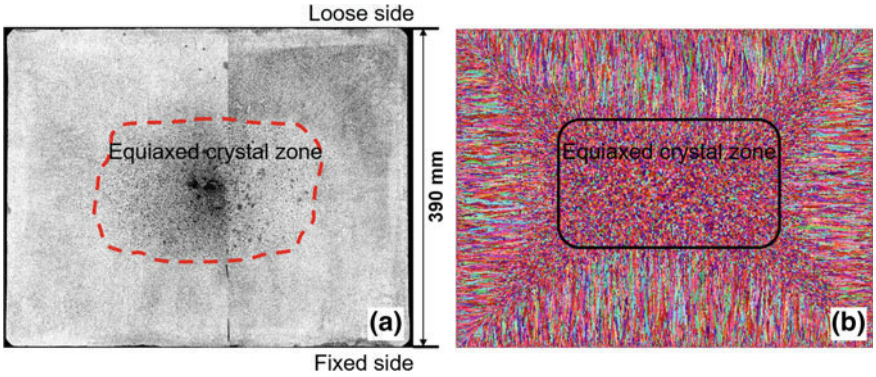

Fig. 2 Simulated and measured solidification structure without M-EMS

was 21.3% and 21.75%, respectively. Both the measured temperature field and the solidification structure agreed well with the numerical results, so the CAFE model was validated for further prediction.

Results and Discussion

To investigate the effect of superheat on the solidification structure, the microstructures of superheat from 15 to 35 °C were calculated, as shown in Fig. 3. The ratio of equiaxed crystal zone and the mean radius of grains under different superheats are shown in Fig. 4. With the superheats increasing from 15 to 35 °C, the ratio of equiaxed crystal zone decreases from 28.47 to 16.45%, and the mean radius of columnar crystal grains becomes larger. However, the mean radius of grains in equiaxed crystal zone is 1.06 mm approximately. So the mean radius of grains in whole section increases from 1.02 to 1.21 mm.

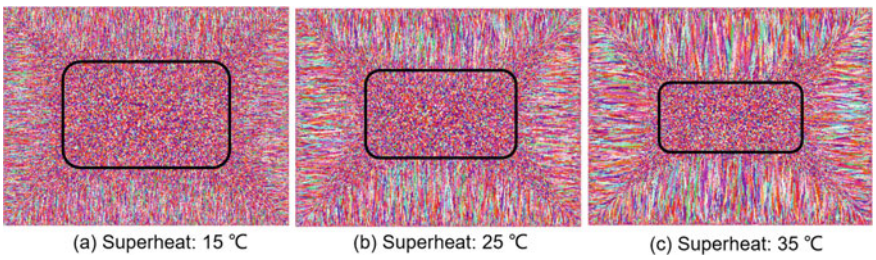

Fig. 3 Effect of superheats on the solidification structure

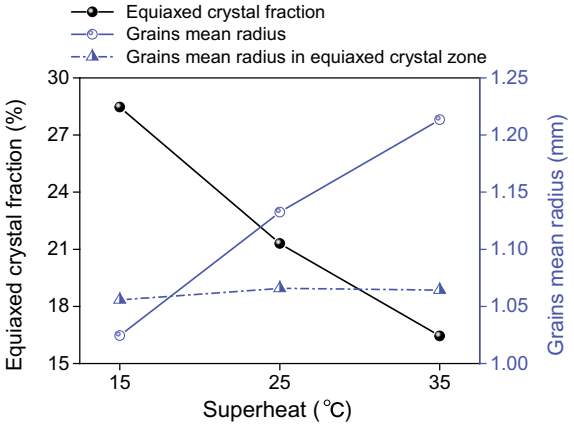

Fig. 4 Ratio of equiaxed crystal zone and mean radius of grains under different superheats

The simulated solidification structure, the ratio of equiaxed crystal zone, and mean radius of grains under different secondary cooling water flow are shown in Figs. 5 and 6. There are three cases including decreasing 20%, normal, and increasing 20% of the secondary cooling water flow. With the secondary cooling water flow increasing, the ratio of equiaxed crystal zone decreases from 23.16 to 20.64%, since enhanced cooling condition contributed to delaying columnar to equiaxed transition (CET). The mean radius of grains in equiaxed crystal zone decreases from 1.09 to 1.06 mm with the secondary cooling water flow increasing. The mean radius of grains in whole section is 1.13 mm approximately.

It has been reported that the mold electromagnetic stirring (M-EMS) plays an important role in improving the surface and inner quality of strand especially improving the ratio of equiaxed crystal zone [13, 14]. Electromagnetic stirring technology employs Lorentz force generated by multi-phase induction coils to stir the molten steel in the mold. The effects of rotating flow induced by electromagnetic force are as follows: increasing heat transfer between the solidification front and molten steel, breaking the dendrites by intense flow field, and increasing the formation of crystals [5, 15]. In current simulation, to simulate the intense flow field and increasing

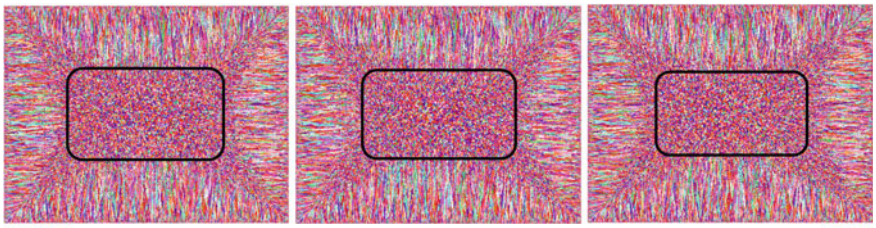

Fig. 5 Effect of secondary cooling water flow on the solidification structure

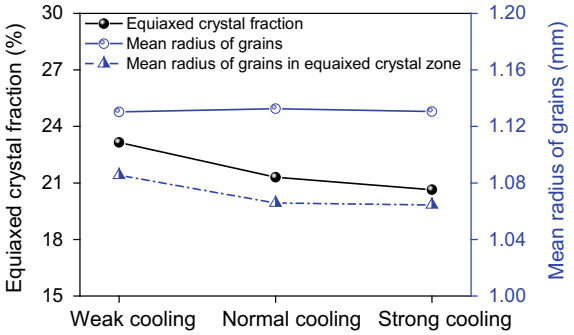

Fig. 6 Ratio of equiaxed crystal zone and mean radius of grains under different secondary cooling water flow

the formation of crystals, the maximum nucleation density of volume was changed from 6.5×10^8 to 7.0×10^8 m^{-3}. As for the increasing heat transfer between the solidification front and molten steel, a 1.2 times thermal conductivity was used with liquid fraction (f_l) larger than 0.7. In the solid zone ($f_l \leq 0.3$), the thermal conductivity remained original value. In the mushy zone with $0.3 \leq f_l \leq 0.7$, the thermal conductivity changed linearly.

The simulated and measured solidification structure with M-EMS is shown in Fig. 7. With the M-EMS considered, the ratio of equiaxed crystal zone increases from 21.75 to 32.77%, and the ratio of equiaxed crystal zone in calculation and industrial experiment was 31.7% and 32.77%, respectively. The results demonstrate that the present model simulating solidification structure formation during the continuous casting process of steel is reliable.

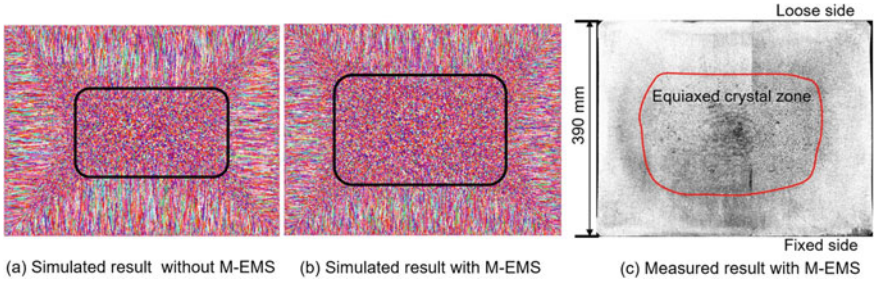

Fig. 7 Simulated solidification structure without M-EMS (**a**) and with M-EMS (**b**), measured solidification structure with M-EMS (**c**)

Conclusions

In the current paper, a coupled cellular automaton-finite element (CAFE) model was used to simulate the solidification structure of continuous casting bloom. The influence of superheat, secondary cooling water flow, and M-EMS on the solidification structure was discussed. The following conclusions can be obtained:

(1) The CAFE model was validated by the measured temperature and solidification structure, and then the CAFE model was reliable for further prediction.
(2) With the superheats increasing from 15 to 35 °C, the ratio of equiaxed crystal zone decreases from 28.47 to 16.45%, and the mean radius of grains increases from 1.02 to 1.21 mm. The mean radius of grains in equiaxed crystal zone is 1.06 mm approximately.
(3) With the secondary cooling water flow increasing, the ratio of equiaxed crystal zone decreases from 23.16 to 20.64%, and the mean radius of grains in equiaxed crystal zone decreases from 1.09 to 1.06 mm. The mean radius of grains in whole section is 1.13 mm approximately.
(4) With the M-EMS considered, the ratio of equiaxed crystal zone increases from 21.75 to 32.77%. The superheat and M-EMS are critical parameters on the solidification.

Acknowledgements The authors are grateful for support from the National Science Foundation China (Grant No. U1860206 and No. 51725402), Beijing International Center of Advanced and Intelligent Manufacturing of High Quality Steel Materials (ICSM), Beijing Key Laboratory of Green Recycling and Extraction of Metals (GREM), and the High Quality Steel Consortium (HQSC) at the School of Metallurgical and Ecological Engineering at University of Science and Technology Beijing (USTB), China.

References

1. Ludlow V, Normanton A, Anderson A (2005) Strategy to minimise central segregation in high carbon steel grades during billet casting. Ironmaking Steelmaking 32(1):68–74
2. Dong Q, Zhang J, Wang B (2016) Shrinkage porosity and its alleviation by heavy reduction in continuously cast strand. J Mater Process Technol 238:81–88
3. Rappaz M, Gandin CA (1993) Probabilistic modelling of microstructure formation in solidification processes. Acta Metall Mater 41(2):345–360
4. Hou Z, Jiang F, Cheng G (2012) Solidification structure and compactness degree of central equiaxed grain zone in continuous casting billet using cellular automaton-finite element method. ISIJ Int 52(7):1301–1309
5. Yamazaki M, Natsume Y, Harada H (2006) Numerical simulation of solidification structure formation during continuous casting in Fe-0.7 mass% C alloy using cellular automaton method. ISIJ Int 46(6):903–908
6. Fang Q, Ni H, Zhang H, Wang B (2017) Numerical study on solidification behavior and structure of continuously cast U71Mn steel. Metals 7(11):483
7. Gandin C-A, Desbiolles J-L, Rappaz M, Thevoz P (1999) A three-dimensional cellular automation-finite element model for the prediction of solidification grain structures. Metall Mater Trans A 30(12):3153–3165